ISSN NO: 9726-001X
Volume 9 Issue 03 2021

JOURNAL OF CURRENT SCIENCE

PLASTIC STRESS-STRAIN PARAMETERS MAY BE IDENTIFIED USING THE VIRTUAL FIELDS APPROACH, TOTAL STRAIN THEORY, AND GLOBAL DIGITAL IMAGE CORRELATION

Suresh Patil.G.L,Chandrakumar.C,Poornima.K

Assoc. Prof,Asst. Prof,Asst. Prof

glspatil@gmail.com, chakrapdit@gmail.com, mechpoornima@gmail.com

Department of Mech,Proudhadevaraya Institute of Technology, Abheraj Baldota Rd, Indiranagar, Hosapete, Karnataka-583225

Abstract

In this study, a method based on virtual fields is suggested for determining plastic constitutive parameters from recorded displacement fields. Measuring using global digital image correlation yields the displacement fields of the specimen surface. Afterwards, piecewise virtual fields are used to perform material property identification. With the total strain theory serving as the constitutive equation, material characteristics may be identified using instantaneous displacement fields. The notion of virtual work is used to derive the relations between material properties, measured displacement fields, measured tractions, and virtual displacements. These connections are then solved numerically to yield the material properties. By using it on displacement fields computed using an elasto-plastic finite element approach and on displacement fields of a pure aluminium specimen collected experimentally, the efficacy of the suggested method is shown. A single set of displacement fields under proportionate loading may identify the elasto-plastic material characteristics, according to the numerical validation findings. Experimental validation findings reveal that elasto-plastic material characteristics may be assessed; nevertheless, a disparity is seen between the directly measured stress-strain curve and the one that is inversely detected.

Key words : Inverse problem, Material properties, Elasto-plastic, Global digital image correlation, Virtual fields method

1. Introduction

Stress and strain analysis is indispensable for assessing structural integrity and for strength evaluation of machines and structures. For such analyses, it is important to know the material properties of the members composing the machines and structures. For example, knowledge of material properties is necessary for finite element stress analysis. In the case of a material exhibiting plastic deformation, the plastic stress-strain properties such as yield stress and hardening parameter and elastic properties should be known. Similarly, knowledge of material properties is necessary for computing stresses from measured strains. Generally, material properties are determined from the stress and strain values obtained through a uniaxial tensile test. However, the actual properties of the materials composing machines and structures are sometimes different from those obtained from the uniaxial tensile test because of various factors such as the heat effect during processing, change in material structures, and work hardening (Miura, 2006). Therefore, the actual properties of such materials are required for performing accurate stress-strain and strength evaluation. Consequently, it is necessary to identify material properties inversely by applying a force on actual machines and structures and measuring their strain output. One inverse method to determine the properties of materials is an indentation technique (Giannakopoulos and Suresh, 1999).

Recently, optical methods such as digital image correlation (Sutton et al., 2009; Yoneyama, 2016) has been widely used to evaluate displacements and strains. These methods yield plenty of data on full-field displacement or strain distribution, and hence, they are effective for identifying material properties through inverse analysis. Consequently,

various methods (Avril et al., 2008a) have been studied for identifying material properties from data measured by optical methods. For example, a method in which an Airy stress function is employed (Hori and Kameda, 2001) and one employing finite element updating (Réthoré, 2010) have been developed. Among these methods (Avril et al., 2008a; Hori and Kameda, 2001; Réthoré, 2010) , the virtual fields method (Grédiac et al., 2009; Grédiac et al., 1994; Grédiac et al., 1999; Pierron and Grédiac, 2000; Moulart et al., 2006; Pierron et al., 2011; Moulart et al., 2011; Grédiac and Pierron 2006; Pannier et al., 2006; Avril et al., 2008a; Sutton et al., 2008) based on the principle of virtual work is one of most widely accepted techniques. This method has been applied to identify the properties of anisotropic materials (Grédiac et al., 2009; Grédiac and Pierron, 2012; Grédiac et al., 1994; Grédiac et al., 1999; Pierron and Grédiac, 2000; Moulart et al., 2006) and materials under dynamic loading conditions (Pierron et al., 2011; Moulart et al., 2011). Elasto-plastic material properties have already been identified by the virtual fields method (Grédiac and Pierron 2006; Pannier et al., 2006; Avril et al., 2008b; Avril et al., 2008c; Sutton et al., 2008; Coppieters et al., 2011; Coppieters et al., 2014; Kim et al., 2014). In these studies (Grédiac and Pierron 2006; Pannier et al., 2006; Avril et al., 2008b; Avril et al., 2008c; Sutton et al., 2008), elasto-plastic material properties were identified from measured displacement data under various loads based on the constitutive relation with the strain incremental theory. Therefore, these methods need a lot of displacement data under various load steps. However, it is convenient to perform identification from a set of displacement distributions under an arbitrary load. In previous study, the authors (Jinno et al., 2014) investigated a method for identifying elasto-plastic material properties from measured data obtained under an arbitrary load using the total strain theory (Hill, 1950) instead of the strain incremental theory. Among measurement methods, digital image correlation has been widely used to obtain displacements as input data for inverse analyses. However, note that the accuracy of measurement results near boundaries is not high in conventional subset-based digital image correlation because subsets overlap the region beyond the boundaries. Therefore, a new method should be used because the region for obtaining data for inverse analysis usually contains boundaries.

This study aims to develop a method for identifying elasto-plastic material properties from a set of displacement fields under a single load, based on the virtual fields method studied in previous study (Jinno et al., 2014). The use of global mesh-based digital image correlation (Yoneyama et al., 2016) is proposed to obtain the displacement fields of the specimen surface because this method yields appropriate results near boundaries and interfaces unlike the conventional subset-based digital image correlation. The Ramberg-Osgood equation (Ramberg and Osgood 1941) is assumed as the stress-strain relation. Then, the relations between displacements, tractions, and virtual displacements are derived by using the total strain theory as the constitutive equation. The effectiveness of the proposed method is demonstrated by identifying the material properties of a pure aluminum specimen under tension. Results show that the proposed method can be used to obtain not only the elastic properties, but also elasto-plastic properties from measured displacement fields.

2. Identification method

2.1 Basic principle of the virtual fields method

Consider that the in-plane displacement distributions of a planar specimen surface are obtained through measurements. Plane stress condition is assumed because the displacements on the surface of the specimen are used for the identification. Based on the principle of virtual work, the following equation can be obtained because the internal virtual work equals the external virtual work in the absence of a body force.

$$\int_{\Omega} \sigma_{ij} \varepsilon_{ij}^{*} \, d\Omega = \int_{\Gamma_q} T_i u_i^{*} \, d\Gamma \qquad (i,j=1,2) \tag{1}$$

where σ_{ij} represents the stress components; ε_{ij}^{*}, the virtual strain components; T_i, the external load components; u_i^{*}, the virtual displacements; Ω, the analysis region; and Γ_q, the boundary that is subjected to the traction. The subscripts i,j = 1, 2 indicate the x and y directions in the Cartesian coordinate system. The stress-strain relationship for a two-dimensional linearly elastic material can be represented as follows:

ISSN NO: 9726-001X
Volume 9 Issue 03 2021

$$\begin{Bmatrix} \sigma_1 \\ \sigma_2 \\ \sigma_6 \end{Bmatrix} = \begin{bmatrix} c_{11} & c_{12} & 0 \\ c_{12} & c_{22} & 0 \\ 0 & 0 & c_{66} \end{bmatrix} \begin{Bmatrix} \varepsilon_1 \\ \varepsilon_2 \\ \varepsilon_6 \end{Bmatrix} \tag{2}$$

where Voigt convention is used; that is, σ_1 and σ_2 are the normal stress components; ε_1 and ε_2, the normal strain components; and σ_6 and ε_6, the shear stress and the shear strain, respectively. In Equation (2), c_{11}, c_{12}, c_{22}, and c_{66} are the elastic constants, and they relate the elastic modulus and the Poisson's ratio. For an isotropic elastic material, the following equation can be obtained from Eqs. (1) and (2).

$$c_{11}\int_{\Omega}\left(\varepsilon_1\varepsilon_1^* + \varepsilon_2\varepsilon_2^* + \frac{1}{2}\varepsilon_6\varepsilon_6^*\right)d\Omega + c_{12}\int_{\Omega}\left(\varepsilon_1\varepsilon_2^* + \varepsilon_2\varepsilon_1^* - \frac{1}{2}\varepsilon_6\varepsilon_6^*\right)d\Omega = \int_{\Gamma_q}\left(T_1u_1^* + T_2u_2^*\right)d\Gamma \tag{3}$$

Herein, the strains ε_1, ε_2, and ε_6 can be obtained by differentiating the measured displacements. The variables u_1^* and u_2^* represent the virtual displacements, and ε_1^*, ε_2^*, and ε_6^* are the virtual strains related to virtual displacement. The loads T_1 and T_2 can be obtained through measurements by using a load transducer. Therefore, the unknowns in Eq. (3) are the two elastic constants c_{11} and c_{12}. Simultaneous equations for these two unknowns can be obtained by introducing two virtual displacements, and then the two unknowns can be obtained by solving these simultaneous equations. This is the basic principle of the virtual fields method. Details of the virtual fields method are available in literature (Grédiac et al., 2009; Grédiac et al., 1994; Grédiac et al., 1999; Pierron and Grédiac, 2000; Moulart et al., 2006; Pierron et al., 2011; Moulart et al., 2011; Grédiac and Pierron 2006; Pannier et al., 2006; Avril et al., 2008a; Avril et al., 2008c; Sutton et al., 2008).

2.2 Identification of elasto-plastic properties by employing the total strain theory

For identifying elasto-plastic material properties, a model of the stress-strain relation is assumed, and the stress and strain relation of a wide range of strain after yielding is obtained by identifying the model parameters. In this study, the Ramberg-Osgood relation (Ramberg and Osgood 1941) that is widely used for representing stress-strain relation of aluminum is used. In this case, the relation between the equivalent stress σ and the equivalent strain ε can be expressed as follows:

$$\varepsilon = \frac{\sigma}{E} + \alpha\frac{\sigma_0}{E}\left(\frac{\sigma}{\sigma_0}\right)^n \tag{4}$$

where E represents the elastic modulus; σ_0, the yield stress; α, the material constant; and n, the hardening index. In the proposed method, a single set of displacement fields obtained under an arbitrary load is used, instead of the multiple measured displacement fields under various loads, as the input data for the inverse analysis algorithm. Thus, the total strain theory (Henkey equations) (Hill, 1950) is used as the constitutive equation instead of the strain incremental theory. Therefore, the proposed method can be applied to proportional loading problems without unloading. By substituting the Ramberg-Osgood equation into the total strain theory, the relation between the stress components σ_{ij} and the strain components ε_{ij} can be expressed as shown in the following equation.

$$\varepsilon_{ij} = \frac{1+\varpi}{E}s_{ij} + \frac{1-2\varpi}{3E}\sigma_{kk}\delta_{ij} + \frac{3}{2}\alpha\varepsilon_0\left(\frac{\sigma}{\sigma_0}\right)^{n-1}\frac{s_{ij}}{\sigma_0} \quad (i,j=1,2) \tag{5}$$

where ϖ represents the Poisson's ratio; δ_{ij}, the Kronecker delta; and s_{ij}, the deviatoric stress components. The relation among the measured strains ε_{ij}, the loads T_i, the virtual displacements u_i^*, the virtual strains ε_{ij}^*, and the material property parameters E, ϖ, α, n, and σ_0 is obtained by substituting Eq. (5) into Eq. (1).

The parameters α, n, and σ_0 are not independent but mutually related. Thus, Eq. (4) is rewritten as follows:

$$\varepsilon = \frac{\sigma}{E} + \beta\sigma^n \tag{6}$$

JOURNAL OF CURRENT SCIENCE

where

$$\beta = \frac{\alpha}{E}\left(\frac{1}{\sigma_0}\right)^{n-1} \tag{7}$$

The parameters σ_0 and α relate the parameters β and n as shown below.

$$\sigma_0 = \sqrt[n]{\frac{0.002}{\beta}} \tag{8}$$

$$\alpha = \beta E \sigma_0^{n-1} \tag{9}$$

when σ_0 represents the proof stress. Thus, the number of unknowns can be reduced by substituting σ_0 and α with β.

Here, consider the case that the elastic modulus E and Poisson's ratio ϖ are known, but the plastic parameters β and n are identified. Because the elastic modulus and the Poisson's ratio are known in many cases and because they are hardly changed by thermal treatment, it is appropriate to treat them as known values. The following equations are obtained for identifying β and n by introducing two virtual displacements.

$$\begin{aligned}
&\int_\Omega \sigma_{11}\varepsilon^{*(1)}\,d\Omega + \int_\Omega \sigma_{22}\varepsilon^{*(1)}\,d\Omega + \int_\Omega \sigma_{66}\varepsilon^{*(1)}\,d\Omega = \int_{\Gamma_q}\left(T_1 u^{*(1)} + T_2 u^{*(1)}\right)d\Gamma \\
&\int_\Omega \sigma_{11}\varepsilon^{*(2)}\,d\Omega + \int_\Omega \sigma_{22}\varepsilon^{*(2)}\,d\Omega + \int_\Omega \sigma_{66}\varepsilon^{*(2)}\,d\Omega = \int_{\Gamma_q}\left(T_1 u^{*(2)} + T_2 u^{*(2)}\right)d\Gamma
\end{aligned} \tag{10}$$

Equation (10) represents nonlinear simultaneous equations for parameters β and n. The Newton–Raphson method is used to obtain them. Equation (10) is then rewritten as follows:

$$f_k = \int_\Omega \sigma_{11}\varepsilon^{*(k)}\,d\Omega + \int_\Omega \sigma_{22}\varepsilon^{*(k)}\,d\Omega + \int_\Omega \sigma_{66}\varepsilon^{*(k)}\,d\Omega - \int_{\Gamma_q}\left(T_1 u^{*(k)} + T_2 u^{*(k)}\right)d\Gamma \tag{11}$$

Herein, k represents the distinction number of the virtual displacement fields (k = 1 and 2). A series of iterative equations based on Taylor's series expansion of Eq. (11) yields the following equations.

$$(f_k)_{i+1} = (f_k)_i + \left(\frac{\partial f_k}{\partial n}\right)\Delta n + \left(\frac{\partial f_k}{\partial \beta}\right)\Delta\beta \tag{12}$$

where subscript i denotes the ith iteration step, and Δn and $\Delta\beta$ are corrections to the previous estimates of n and β. The desired results $(f_k)_{i+1} = 0$ yield the following simultaneous equations with respect to the corrections.

$$-f_k = \left(\frac{\partial f_k}{\partial n}\right)\Delta n + \left(\frac{\partial f_k}{\partial \beta}\right)\Delta\beta \tag{13}$$

Equation (13) can be rewritten in matrix form as follows:

$$\mathbf{f} = \mathbf{b}\Delta \tag{14}$$

where

$$\mathbf{f} = \begin{Bmatrix} -f_1 \\ -f_2 \end{Bmatrix},\ \mathbf{b} = \begin{bmatrix} \dfrac{\partial f_1}{\partial n} & \dfrac{\partial f_1}{\partial \beta} \\ \dfrac{\partial f_2}{\partial n} & \dfrac{\partial f_2}{\partial \beta} \end{bmatrix},\ \Delta = \begin{Bmatrix} \Delta n \\ \Delta\beta \end{Bmatrix} \tag{15}$$

ISSN NO: 9726-001X
Volume 9 Issue 03 2021

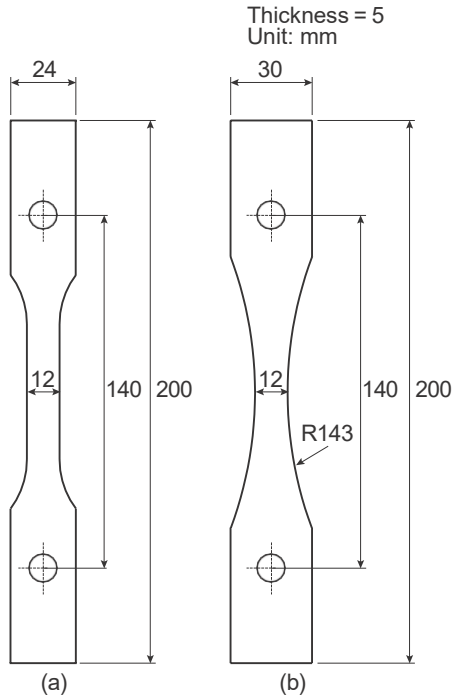

Fig. 1 Specimen geometries: (a) uniaxial test; (b) identification by virtual fields method

The solution for Eq. (14) is as follows:

$$\Delta = \mathbf{b}^{-1}\mathbf{f} \tag{16}$$

The solution of the matrix equation gives the correction terms for prior estimates of parameters n and β. Accordingly, an iterative procedure must be used to obtain the parameters. Then, the estimates of the unknowns are revised. The procedure is repeated until the corrections become acceptably small. Finally, the parameters σ_0 and α are obtained from the values of n and β. Equation (15) indicates that the derivatives of f_k with respect to the unknowns are required in matrix **b**. However, the values of stresses σ_1, σ_2, and σ_6 in Eq. (11) can be obtained by solving Eq. (5) numerically; Eq. (11) cannot be represented as the function of the unknowns. Therefore, the derivatives of f_k are obtained by numerical differentiation.

In this study, the virtual fields method is implemented with piecewise virtual fields (Toussaint et al., 2006). That is, a finite element model of the analysis region is produced, the measured displacements, the virtual displacements, and the tractions are assigned to the nodes of the model, and then, the domain and boundary integrals are computed numerically.

3. Experimental verification of the proposed method

3.1 Procedure for experiment and inverse analysis

Material property identification is performed to verify the proposed method. The material used in the experiment is annealed pure aluminum A1050. Two types of the specimen are prepared as shown in Fig. 1. The specimen shown in Fig. 1(a) is used for a uniaxial tension test to plot the stress-strain diagram that is used as reference data to verify the identification results. In the uniaxial tension test, strains are measured using strain gauges. Identification by the proposed method is applied to the displacement fields of the specimen shown in Fig. 1(b). For digital image correlation, the specimen is painted with black ink on the surface, and a white dot pattern is overlaid by spray painting, creating a speckle-like pattern. The size of the random pattern is selected to oversample the intensity pattern using several sensors for accurate measurement. In this study, each random pattern is oversampled by 10–40 pixels. The variations in the speckle-like pattern on the specimen are observed by a monochromatic CCD camera (2048 × 2048 pixels × 8 bits) equipped with a telephoto lens with a focal length of 200 mm. The length of 1 mm corresponds to

ISSN NO: 9726-001X
Volume 9 Issue 03 2021

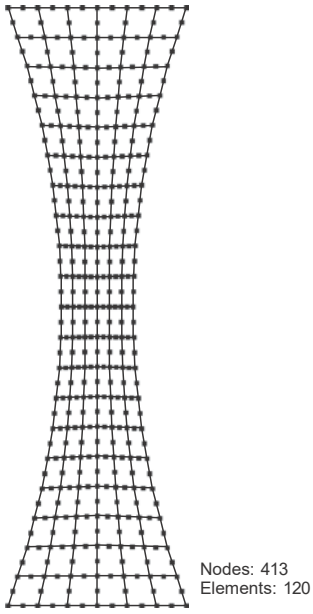

Fig. 2 Finite element model for displacement measurement by global digital image correlation and identification by the virtual fields method

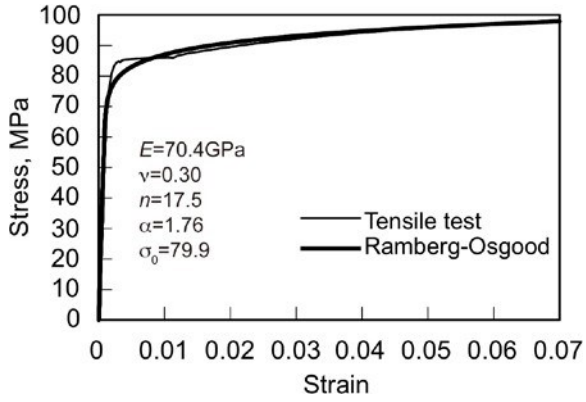

Fig. 3 Stress-strain diagram for annealed aluminum alloy and the curve approximated by using the Ramberg-Osgood equation

about 18 pixels on an image. Various algorithms have been proposed for digital image correlation. In this study, a global digital image correlation algorithm (Yoneyama et al., 2016) employing a finite element mesh to search for displacements at all nodes simultaneously is used. Figure 2 shows the finite element model for global digital image correlation used in this study. The model consists of 8-noded isoparametric elements. A bicubic interpolation method is used for obtaining the continuous speckle pattern. The data processing is implemented using software developed by one author.

The domain and boundary integrals included in the inverse analysis method are processed using the same finite element model as the displacement measurement with global digital image correlation. It is sometimes difficult to obtain appropriate results by inverse analysis because of the errors in strains attributed to the differentiation of the measured displacements. Therefore, the displacement fields are smoothed by minimizing the sum of the residuals of the measured and smoothed displacements and the second-order derivatives of the approximated values (Yoneyama, 2016). Furthermore, the strains obtained by numerical differentiation using a finite element are smoothed similarly. Then, the nodal displacements are determined by minimizing the sum of the residuals of the measured and smoothed strains and those of the smoothed strains and the strains obtained from the smoothed displacements. The values of the measured and virtual displacements, and strains at integration points inside elements are obtained from the nodal values. Then, the integrations included in the inverse analysis are computed. In iterative computation, realistic

ISSN NO: 9726-001X
Volume 9 Issue 03 2021

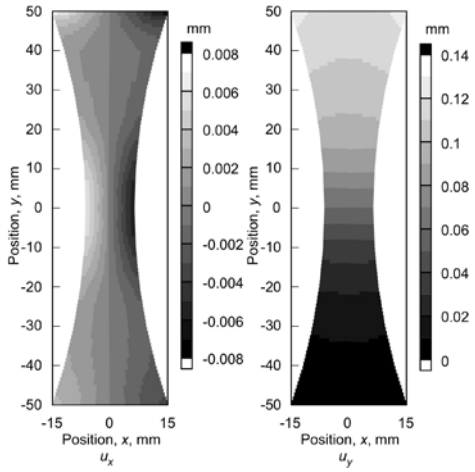

Fig. 4 Displacement distributions obtained by elasto-plastic finite element analysis (P = 4900 N)

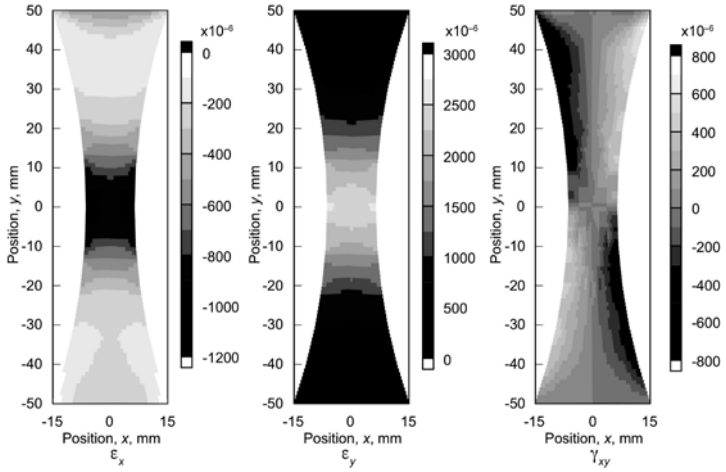

Fig. 5 Strain distributions obtained by elasto-plastic finite element analysis (P = 4900 N)

values for pure aluminum, i.e., α = 1.8, n = 12, and σ_0 = 75 GPa, are used as the initial values, and the convergence is judged when the absolute values of the corrections are less than 0.01.

3.2 Results and discussion

Figure 3 shows the true stress and true strain diagram obtained through the uniaxial tension test of the specimen shown in Fig. 1(a). The approximated curve obtained by the Ramberg-Osgood relation (Ramberg and Osgood, 1941) is also shown. Although the difference between the measured and approximated curves can be observed around the yielding stress, the representation of the stress-strain relation, except around the yielding stress, by the Ramberg-Osgood equation is in good agreement with the actual data. As described in the previous section, in the proposed method, the parameters in the Ramberg-Osgood relation are identified, and then, the approximated stress-strain curve is obtained.

Before applying the proposed method to experimentally obtained displacement fields, the identification is performed from the displacement fields obtained by an elasto-plastic finite element method to validate the proposed procedure and software developed in this study. The experiment described in previous subsection is simulated and the displacement fields are obtained by finite element analysis using commercial software of MSC Marc 2014. Figure 4 shows the displacement distributions obtained using the finite element method under the load of P = 4900 N and the corresponding strains are shown in Fig. 5. The virtual displacements are established manually as described later. The elastic parameters of E = 70.4 GPa and ϖ = 0.3 are used as the known material properties. Then, the plastic

ISSN NO: 9726-001X
Volume 9 Issue 03 2021

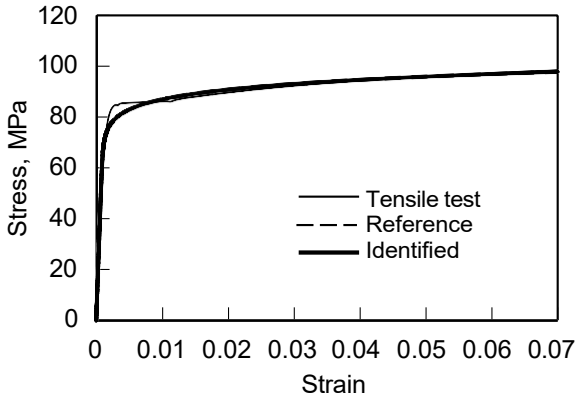

Fig. 6 Stress-strain diagrams identified from displacement fields obtained by finite element analysis

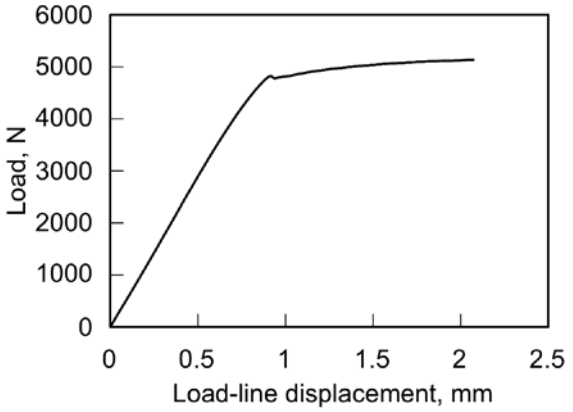

Fig. 7 Load and load-line displacement curve

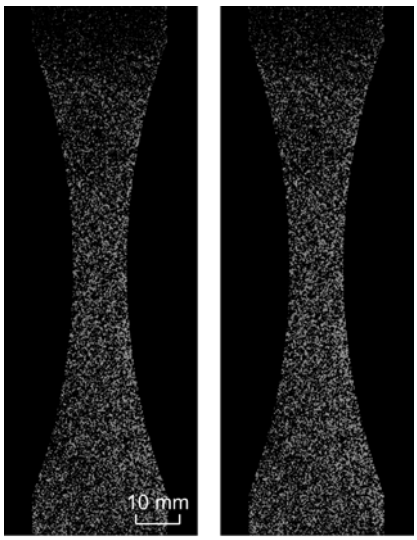

Fig. 8 Images of the specimen surface: (a) reference; (b) after deformation (P = 3600 N)

parameters are identified. The identified parameters are α = 1.76, n = 17.5, and σ_0 = 79.9. The stress-strain curve constructed from the identified parameters is shown in Fig. 6 together with the curve obtained by the tensile test. As shown in this figure, the identified stress-strain curve agrees with the curve by the tensile test. The values of the identified parameters coincide with those obtained by a least-squares method shown in Fig. 3. That is, the

ISSN NO: 9726-001X
Volume 9 Issue 03 2021

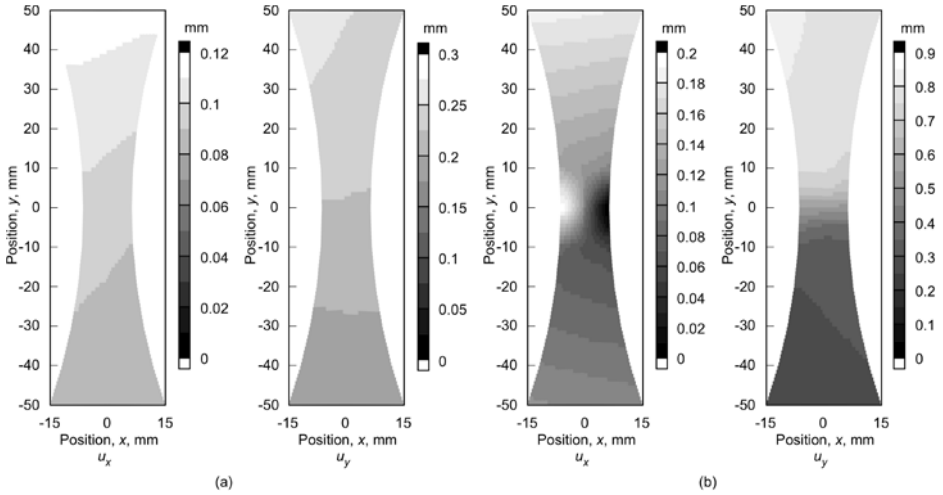

Fig. 9 Displacement distributions obtained by global digital image correlation: (a) P = 3600 N; (b) P = 5000 N

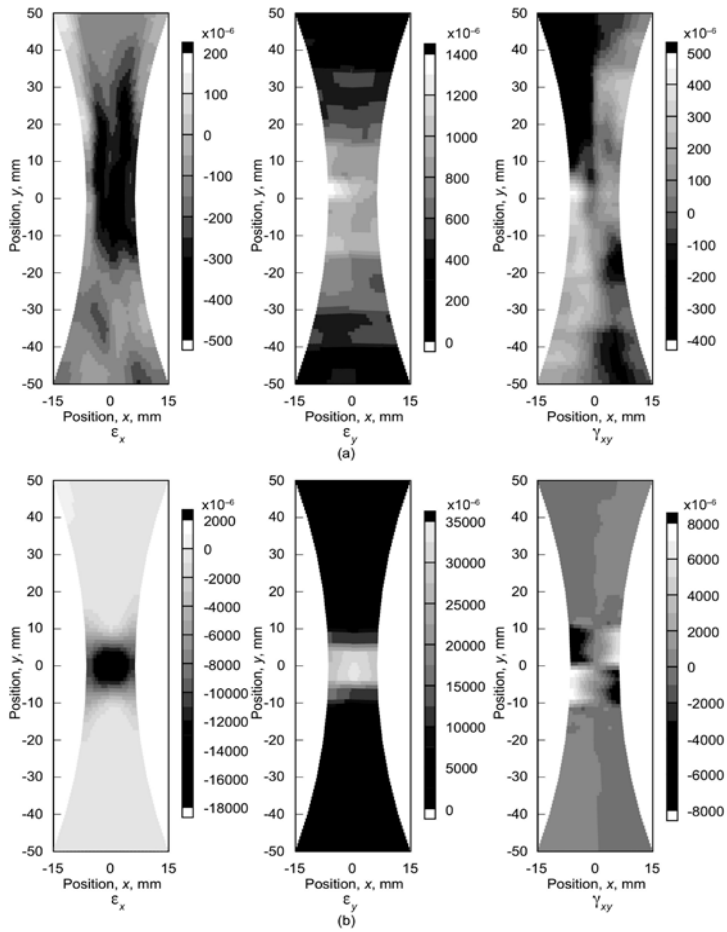

Fig. 10 Strain distributions obtained by global digital image correlation: (a) P = 3600 N; (b) P = 5000 N

elasto-plastic material properties can be obtained from a single set of the displacement fields using the total strain theory in the virtual fields method.

Figure 7 shows the relation between the load and the loading point displacement of the specimen shown in Fig.

1(b). The elastic region and the region where the material exhibits yielding and the plastic deformation can be clearly identified in Figure 7. The identification results for the elastic displacement fields under a load of P = 3600 N and the plastic deformation fields under a load of P = 5000 N are mainly described in the following text.

Figure 8 shows the photographs of the specimen surfaces before and after a load of P = 3600 N is applied. The 650 × 2048 pixel regions of the 2048 × 2048 pixel images are shown in this figure. The random pattern created by spraying black and white paints can be observed. However, the deformation of the specimen cannot be recognized from these figures. The mesh-based global digital image correlation is applied to these images to obtain displacement distributions. Strain distributions are also obtained by differentiating the displacements with the manner in ordinarily finite element analysis. The results of displacement and strain measurements are shown in Figs. 9 and 10, respectively. As shown in Fig. 9(a), there is a gradual variation in the displacement before the specimen exhibits plastic deformation. Meanwhile, the displacement varies suddenly at the middle part of the specimen after the plastic deformation, as shown in Fig. 9(b). The uniform strain distributions reflecting these displacement distributions are shown in Fig. 10(a), and the strain concentration at the center of the specimen is observed in Fig. 10(b).

First, the elastic modulus and the Poisson's ratio are identified from the displacement fields under various loads assuming elastic deformation. For identifying elastic properties using the virtual fields method, virtual displacements can be automatically established to minimize the effect of the measurement errors (Moulart et al., 2006; Avril et al., 2004). In this study, the virtual displacements are automatically determined by applying this method, and then the elastic modulus and the Poisson's ratio are determined. The identified values for various loads are shown in Fig. 11. The identified elastic moduli and the Poisson's ratios under loads of less than 4000 N are approximately E = 68 GPa and ϖ = 0.28, respectively. These values are appropriate as the material properties of pure aluminum. In addition,

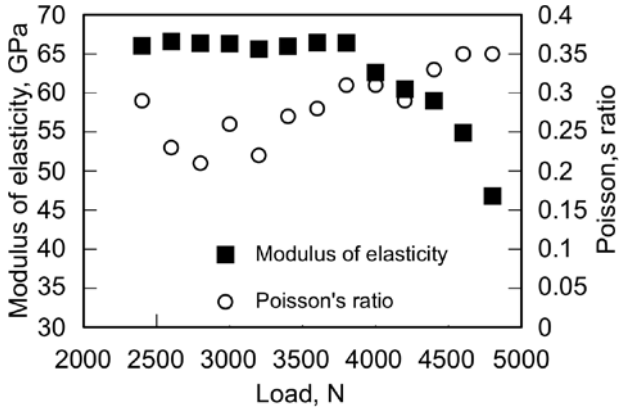

Fig. 11 Identified elastic modulus and Poisson's ratio under various loads

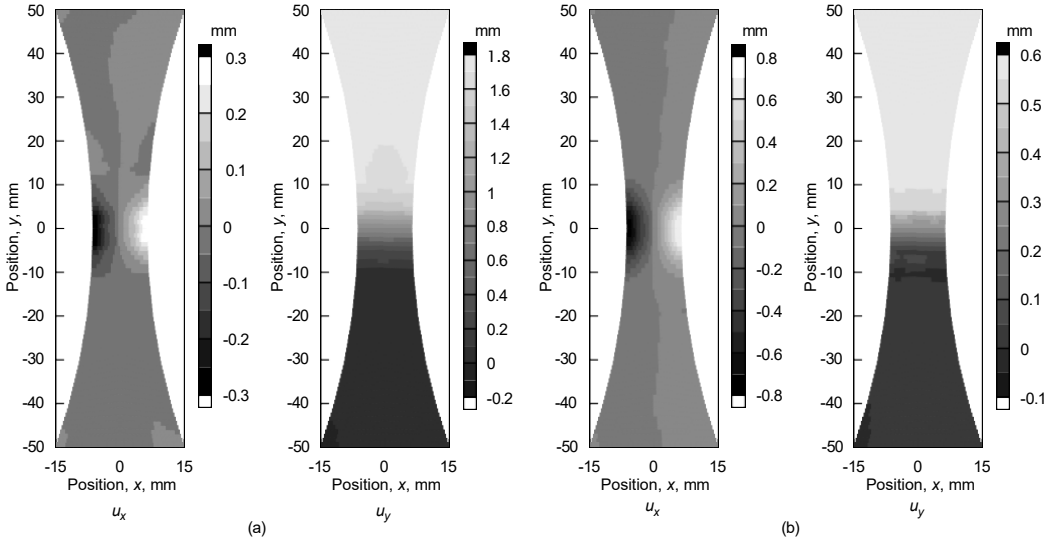

Fig. 12 Virtual displacement fields for identifying plastic parameters: (a) $\mathbf{u}^{*(1)}$; (b) $\mathbf{u}^{*(2)}$

ISSN NO: 9726-001X
Volume 9 Issue 03 2021

the values show good agreement with those obtained by the uniaxial tension test, as shown in Fig. 3. However, the value of the elastic modulus decreases with the increase in the load when the load is higher than P = 4000 N. This is attributed to the fact that the apparent elastic modulus decreases because strains exhibit a high value after yielding, but the identification is performed assuming elastic deformation. Therefore, the material yields under a load of 4000 N, that is, the nominal stress of 67 MPa. The stress-strain diagram shown in Fig. 3 indicates that the material yielding under a load of approximately 4000 N is appropriate.

Next, the plastic properties are identified by the proposed method. The appropriate virtual displacements cannot be established automatically in this case, because the equations connecting the unknown material properties with other parameters are nonlinear, unlike in the case of the elastic material. Thus, the virtual displacements have to be established manually, as shown in Fig. 12. The identified elastic parameters of E = 68 GPa and ϖ = 0.28 are used as the known material properties. Table 1 lists the identified parameters α, σ_0, and n under the loads of 5000 and 5200

Table 1 Identified plastic parameters

	n	α	σ_0, MPa
Identified (P = 5000 N)	7.18	2.03	69.24
Identified (P = 5200 N)	6.44	2.18	64.46

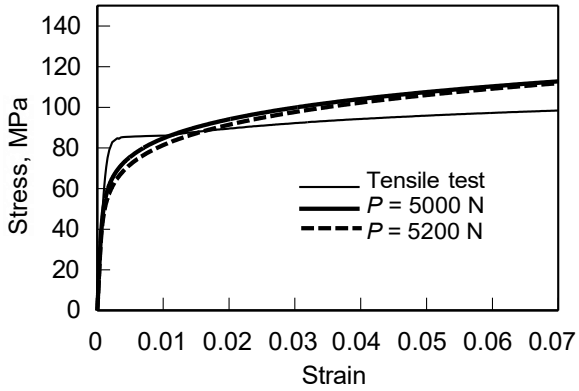

Fig. 13 Identified stress-strain diagrams with known elastic modulus and Poisson's ratio

Table 2 Identified plastic parameters and elastic modulus

	E, GPa	n	α	σ_0, MPa
Identified (P = 5000 N)	58.5	5.89	20.2	58.02
Identified (P = 5200 N)	53.3	4.93	19.2	55.45

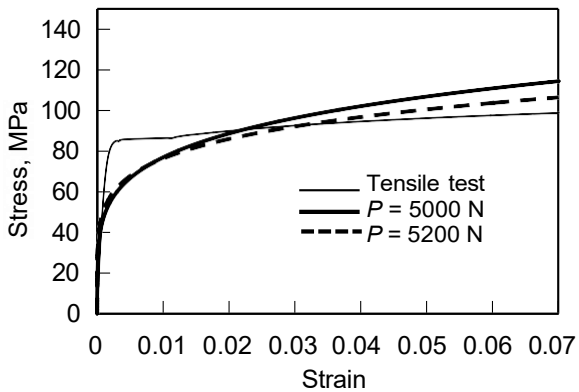

Fig. 14 Identified stress-strain diagrams with known Poisson's ratio

N, and Fig. 13 shows the stress-strain diagrams. Table 1 and Fig. 3 indicate that the identified plastic parameters differ from those obtained by the tensile test, whereas the identified stress-strain curves in Fig. 13 show fairly good agreement with the tensile test results. In order to evaluate the difference between the identified results and the tensile test, the area under the curve is computed, and the ratios are evaluated as the error. In addition, the coefficient of the determination (R^2 value) is evaluated to determine the correlation between the curves. The error is found to be 4.0%, and the coefficient of the determination is 0.984 for a load P = 5000 N; similarly, the error is 3.3 % and the coefficient is 0.961 for a load P = 5200 N. The proposed method does not use the variation in the displacements; instead, the displacements at an instant under arbitrary load are employed. Therefore, highly accurate identification is not expected, but identification is possible, as inferred from the results described above.

Finally, not only the plastic parameters α, σ_0, and n, but also the elastic modulus E are identified simultaneously. Only Poisson's ratio is assumed as the known value. Three virtual displacements are considered because three unknowns—E, β, and n—are involved. The results are presented in Table 2 and Fig. 14. Low values of the elastic modulus are obtained, but the stress-strain curves obtained are reasonable. The errors are 2.0% and 1.7 % for loads of 5000 N and 5200 N, respectively, and the corresponding coefficients of the determination are 0.929 and 0.916, respectively. Thus, it is possible to identify the plastic parameters and the elastic modulus. An attempt is made to identify four parameters with the Poisson's ratio as an unknown; however, converging solution for the nonlinear equation cannot be obtained.

The results of this study show that the proposed method can be used to identify the elasto-plastic material properties from the measured displacement fields obtained at an instant. However, highly accurate identification is not possible at this stage. Further study is required to realize highly accurate identification.

4. Conclusions

We provide a technique to extract elasto-plastic material characteristics from displacement fields recorded under any given load. The suggested technique use instantaneous displacement fields rather than those that exhibit variation. Applying the suggested approach to the displacement fields of a pure aluminium specimen acquired using global digital image correlation demonstrates its efficiency. A single set of displacement fields under proportionate loading may identify the elasto-plastic material characteristics, according to the numerical validation findings. Experimental validation findings reveal that elasto-plastic material characteristics may be assessed; nevertheless, a disparity is seen between the directly measured stress-strain curve and the one that is inversely detected. The remaining differences can only be completely understood with further investigation. Improving the suggested technique is anticipated to allow for the identification of material qualities of elements forming real buildings.

Acknowledgment

This work was supported by JSPS KAKENHI Grant Number 26420024.

References

Avril, S., Bonnet, M., Bretelle, A.-S., Grédiac, M., Hild, F., Ienny, P., Latourte, F., Lemosse, D., Pagano, S., Pagnacco, E. and Pierron, F., Overview of identification methods of mechanical parameters based on full-field measurements, Experimental Mechanics, Vol. 48 (2008a), pp. 495–508.

Avril, S., Grédiac, M. and Pierron, F., Sensitivity of the virtual fields method to noisy data, Computational Mechanics, Vol. 34 (2004), pp. 439–452.

Avril, S., Pierron, F., Pannier, Y. and Rotinat, R., Stress reconstruction and constitutive parameter identification in plane-stress elasto-plastic problems using surface measurements of deformation fields, Experimental Mechanics, Vol. 48 (2008b), pp. 403–419.

Avril, S., Pierron, F., Sutton, M.A. and Junhui, Y., Identification of Elasto-visco-plastic parameters and characterization of lüders behavior using digital image correlation and the virtual fields method, Mechanics of Materials, Vol. 40 (2008c), pp. 729–742.

Coppieters, S., Cooreman, S., Sol, H., Van Houtte, P. and Debruyne, D., Identification of the post-necking hardening behaviour of sheet metal by comparison of the internal and external work in the necking zone, Journal of Materials Processing Technology, Vol. 211 (2011), pp. 545–552.

Coppieters, S. and Kuwabara, T., Identification of post-necking hardening phenomena in ductile sheet metal, Experimental Mechanics, Vol. 54 (2014), pp. 1355–1371.

Giannakopoulos, A.E. and Suresh, S., Determination of elastoplastic properties by instrumented sharp indentation, Scripta Materialia, Vol. 40 (1999), pp. 1191–1198.

Grédiac, M., Pierron, F., Avril, S. and Toussaint, E., The virtual fields method for extracting constitutive parameters form full-field measurements: a review, Strain, Vol. 42 (2006), pp. 233–253.

Grédiac, M., Pierron, F. and Vautrin, A., The iosipescu in-plane shear test applied to composites: a new approach based on displacement field processing, Composites Science and Technology, Vol. 51 (1994), pp. 409–417.

Grédiac, M., Pierron, F. and Surrel, Y., Novel procedure for complete in-plane composite characterization using a single t-shaped specimen, Experimental Mechanics, Vol. 39 (1999), pp. 142–149.

Grédiac, M. and Pierron, F., Applying the virtual fields method to the identification of elasto-plastic constitutive parameters, International Journal of Plasticity, Vol. 22 (2006), pp. 602–627.

Hill. R., The Mathematical Theory of Plasticity (1950), p. 45, Oxford University Press.

Hori, M. and Kameda, T.: Inversion of stress from strain without full knowledge of constitutive relations, Journal of the Mechanics and Physics of Solids, Vol. 49 (2001), pp. 1621–1638.

Jinno, K., Arikawa, S., Yoneyama, S., Watanabe, Y., Asai, T., Shiokawa, K. and Yamashita, M., Identification of elasto-plastic material properties with full-field surface displacement measurements, Journal of the Japanese Society for Experimental Mechanics, Vol. 14 (2014), pp. s147–s152.

Kim, J.H., Serpanti, A,, Barlat, F., Pierron, F. and Lee, M.G. Characterization of the post-necking hardening behaviour using the virtual fields method, International Journal of Solids and Structures, Vol. 50 (2013), pp. 3829–3842.

Miura, H., Materials and mechanics in nano scale, Transactions of the Japan Society of Mechanical Engineers, Series A, Vol. 72, (2006), pp. 595–601 (in Japanese).

Moulart, R., Avril, S. and Pierron, F., Identification of the through-thickness rigidities of a thick laminated composite tube, Composites Part A, Vol. 37 (2006), pp. 326–336.

Moulart, R., Pierron, F., Hallett, S.R. and Wisnom, M.R., Full-Field strain measurement and identification of composites moduli at high strain rate with the virtual fields method, Experimental Mechanics, Vol. 51 (2011), pp. 509–536.

Pannier, Y., Avril, S., Rotinat, R. and Pierron, R., Identification of elasto-plastic constitutive parameters from statically undetermined tests using the virtual fields method, Experimental Mechanics, Vol. 46 (2006), pp. 735–755.

Pierron, F. and Grédiac, M., Identification of through-thickness moduli of thick composites from whole-field measurements using the iosipescu fixture: theory and simulations, Composites Part A, Vol. 31 (2000), pp. 309–318.

Pierron, F., Sutton, M.A. and Tiwari, V., Ultra high speed DIC and virtual fields method analysis of a three point bending impact test on an aluminium bar, Experimental Mechanics, Vol. 51 (2011), pp. 537–563.

Ramberg, W. and Osgood, W.R., Description of stress-strain curves by three parameters, Technical Note No. 902 (1941), National Advisory Committee for Aeronautics.

Réthoré, J., A Fully integrated noise robust strategy for the identification of constitutive laws from digital images, International Journal for Numerical Methods in Engineering, Vol. 84 (2010), pp. 631–660.

Sutton, M.A, Orteu, J.-J. and Schreier, H.W., Image Correlation for Shape, Motion and Deformation Measurements (2009), Springer.

Sutton, M.A., Yan, J.H., Avril, S., Pierron, F. and Adeeb, S.M., Identification of heterogeneous constitutive parameters in a welded specimen: uniform stress and virtual fields methods for material property estimation, Experimental Mechanics, Vol. 48 (2008), pp. 451–464.

Toussaint, E, Grédiac, M and Pierron, F., The virtual fields method with piecewise virtual fields, International Journal of Mechanical Sciences, Vol. 48 (2006), pp. 256−264.

Yoneyama, S., Basic principle of digital image correlation for in-plane displacement and strain measurement, Advanced Composite Materials, Vol. 25 (2016), pp. 105–123.

Yoneyama, S., Koyanagi, J. and Arikawa, S.: Measurement of discontinuous displacement/strain using mesh-based digital image correlation, Advanced Composite Materials, Vol. 25 (2016), pp. 329–343.